

# Interaction of antibiotics Lasalocid and Monensin with model membranes evidenced by Raman spectroscopy and FT-IR

Michel Picquart\*

*Departamento de Física, Universidad Autónoma Metropolitana Iztapalapa  
Apartado postal 55-534, 09340 México D.F., Mexico*

Recibido el 26 de febrero de 1999; aceptado el 29 de noviembre de 1999

Perturbations induced by Lasalocid and Monensin as sodium salts on molecular organization of two types of model membranes prepared with a lipid, dipalmitoylphosphatidylcholine (DPPC) and a surfactant, cetyltrimethylammonium bromide (CTAB) have been analyzed by Raman and infrared spectroscopies. Our approach involves the possible changes in the vibrational spectrum of lipid multilayers for different molar ratios around the order-disorder transition temperature ( $T_m$ ) and changes in the vibrational spectrum of a micellar solution of CTAB (20% by weight) in the  $\text{CH}_2$  stretching vibration modes for different molar ratios. In the hydrophobic core of the multilayer membrane, the interaction of Lasalocid is associated with changes in lipid packing. With DPPC, an effect is detected which corresponds to a decrease of the chain packing of the lipid. In presence of this antibiotic, the transition temperature  $T_m$  decreases depending on the lipid: antibiotic molar ratio. Effect of Monensin is quite different, the transition temperature is not modified by increasing concentrations of this antibiotic. Evidence of penetration of Lasalocid inside the lipid core of the membrane is given. Penetration of Monensin is discussed.

*Keywords:* Raman; FTIR; model membranes; lasalocid; monensin

Perturbaciones inducidas por las sales de sodio de lasalócido y monensina en la estructura molecular de dos tipos de membrana modelos preparados con un lípido, (DPPC) y un tensioactivo (CTAB) se analizaron por espectroscopías Raman e infrarroja. Nuestro enfoque toma en cuenta posibles cambios en el espectro vibracional de las multicapas de lípido a diferentes fracciones molares alrededor de la temperatura de transición orden-desorden ( $T_m$ ), así como cambios en el espectro vibracional de una solución micelar de CTAB (20% en masa) en los modos de vibración de elongación de los grupos  $\text{CH}_2$ . En la parte hidrófoba de la membrana la interacción del lasalócido est asociada con cambios en el apilamiento de los lípidos. Con DPPC, se observa una disminución del apilamiento de las cadenas del lípido. En presencia del antibiótico, la temperatura de transición  $T_m$  disminuye dependiendo de la razón molar lípido antibiótico. El efecto de la monensina es muy diferente, la temperatura de transición no cambia con la concentración del antibiótico. Se observa claramente la penetración del lasalócido dentro de la parte hidrófoba de la membrana. Finalmente, se discute la ubicación de la monensina.

*Descriptores:* Raman; FTIR; membrana modelos; lasalócido; monensina

PACS: 87.15.By; 87.15.Mi; 78.30.-j

## 1. Introduction

Lasalocid and Monensin are polyether carboxylic ionophores which have been extensively studied by X-ray diffraction methods [1-5]. Usually, they form monomeric or dimeric structures, with a preference for the second ones in non-polar solvents, and the metal ion is bonded through oxygen functional groups. They have received much attention because of their ability to transport metal cations across membranes (natural or artificial). It is generally believed [6-8] that Lasalocid and Monensin form specific complexes with cations via hydrogen bonds and encircle the cation (Las-Na, Mon-Na), which becomes lipophilic, and provides a mean to cross membranes. Molecular formulas of both antibiotics are presented in Fig. 1. Such complexes are formed at the interface between lipid and water and they are driven across the bilayer by gradients in cation concentration and pH. One difference between the two ionophores is seen from their transport selectivity that have been extensively studied [9-14]. Lasalocid seems most efficient for carrying  $\text{K}^+$  ions and Monensin for  $\text{Na}^+$  ions. The antibiotic activity of these molecules probably

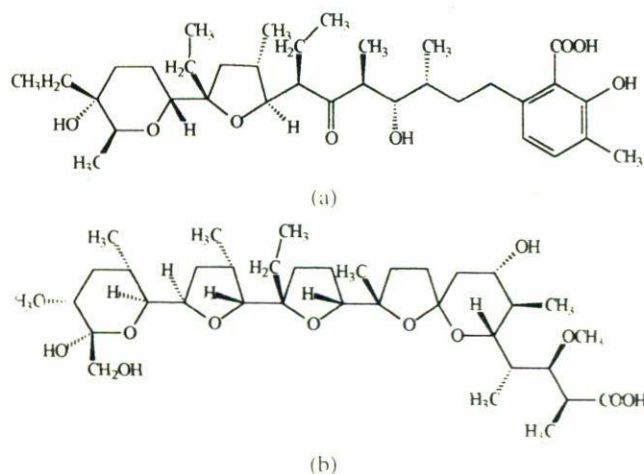


FIGURE 1. Molecular formulas of a) Lasalocid, and b) Monensin.

arises from the carrier mechanism. Circular dichroism has been performed [15] and has shown the formation of a complex between the carboxylate ion of Las-Na anion and the alkylammonium ion.

Less attention has been drawn on interaction with phospholipids. Some works on fluorescence have been performed using the intrinsic fluorescence of Las-Na [7, 16]. These results have been interpreted in terms of limited solubility of Lasalocid A in the phospholipid vesicles, this solubility being higher in fluid than in rigid phospholipid. Also, these results have shown, that at low lipid : Las-Na molar ratio (lower than 50:1), Las-Na has a tendency to form aggregates so as to minimize the exposure of its hydrophilic portion to the hydrophobic interior of the lipid bilayer. In a recent work, Hasmonay *et al.* [17] also interpret their results of Langmuir films of lipids-antibiotic by the formation of aggregates, but also suggest the possibility of penetration of the antibiotic molecules inside the lipid chains region at molar ratio lower than 25:1. It was recently shown [18] an aggregation tendency more important for Mon-Na than for Las-Na, but also enhanced by the basic pH. This work concluded that Las-Na molecules must be situated to some extent inside the lipid bilayer.

Differential scanning calorimetry (DSC) was performed [19] in order to study insertion properties of Las-Na and Mon-Na in DPPC multilamellar bilayers. It was shown that the gel-liquid crystalline phase transition is concentration dependent with Las-Na while not with Mon-Na.

In order to elucidate the membrane damage resulting from the interaction with the antibiotic we have undertaken, by spectroscopic techniques, a comparative analysis of model membranes containing DPPC or DPPC/antibiotic (Las-Na or Mon-Na) in two aqueous solutions: water at pH 6 and at pH 9. High concentrations  $r$  of antibiotics ( $r$  = molar ratio lipid/antibiotic, 100:1, 50:1, 28:1 and 10:1) are chosen because, in poultry, antibiotics are added to medicated animal feeds at 100 mg kg<sup>-1</sup> for the treatment of coccidiosis. Residue levels of 0.005 mg kg<sup>-1</sup> are encountered in tissues [20]. We completed this work, studying the effect of both antibiotics ratios ( $r$  = 50:1, 20:1, 10:1 and 5:1) on a 20% micellar solution of cetyltrimethylammonium Bromide (CTAB).

## 2. Materials and methods

Sodium salt of Lasalocid (97%) and Monensin (90–95%) and DPPC (> 99% by TLC) were purchased from Sigma. CTAB is a cationic surfactant and was purchased from Merck. Las-Na was recrystallized from aqueous methanol and acetone, m.p. 169–172°C. Mon-Na was recrystallized from aqueous methanol and diethoxyde, m.p. 260–264°C. The solvents were Prolabo analytical grade. Chloroform and hexane were distilled on molecular sieve 4 Å for moisture removal. Water was purified in a Bioblock four cartridge system. Heavy water was purchased from Euriso-top (CEA) with 99.8% of deuterium.

Lasalocid and Monensin sodium salts are poorly soluble in water and were first dissolved in a chloroform-hexane solution (2:3, v:v) then DPPC is added to reach the desired concentration. The solvent is then evaporated from the liquid mixture during 10 min at 60°C. The residue is then

dried under vacuum at 37°C favored by a hot-cold current. DPPC/antibiotic mixtures at molar ratios 10:1, 28:1, 50:1 and 100:1 were prepared using this method [25]. The same technique was used to prepare CTAB/antibiotic mixtures at molar ratios 5:1, 10:1, 20:1 and 50:1. It must be noticed here that samples of CTAB/Mon-Na at 5:1 were not obtained because an aggregation process has been occurring in the solution. The same aggregation process occurs in the others mixtures of Mon-Na with time. It must be noted that dissolution of both antibiotics in an anionic surfactant solution as sodium dodecyl sulfate or sodium octanoate is impossible.

For Infrared measurements, samples were obtained by dissolving 2 mg of powder in 40 ml of distilled water or heavy water. Films of hydrated systems were then placed directly between CaF<sub>2</sub> windows with an optical pathway of 7 μm. Spectra were recorded on a Nicolet 5DX spectrometer equipped with a TGS detector. In order to eliminate spectral contributions of atmosphere water vapor, the instrument was purged with dry air. For each spectrum, 100 scans at 4 cm<sup>-1</sup> resolution were collected, co-added, apodized with a Happ-Genzel function and Fourier transformed. The spectra of the solvents were subtracted from the spectra of the solution in particular for lower concentration solutions.

For Raman spectroscopy experiments, all the samples were prepared dissolving 4 mg of powder in 30 ml of water, heated and mixed above the transition temperature. The Raman spectroscopy experiments were performed on a computerized Jobin-Yvon Ramanor HG2S double monochromator, using a 2016 Spectra Physics Ar<sup>+</sup> laser. We used 514.5 nm laser line with a power of 200 mW at the laser head and the spectral resolution was nearly 4 cm<sup>-1</sup>. All the samples were enclosed into sealed 1 mm diameter capillaries and placed in a small cryostat with nitrogen circulation and temperature regulation for the temperature experiments. For technical reasons, the platin resistor was quite far from the focusing point of the laser beam, and the error in temperature measurements was estimated to be ± 0.5°C. The sample was allowed to reach thermal equilibrium for 15 min. before recording each spectrum. For each spectrum at least 10 scans were collected and co-added in order to have a good signal to noise ratio it is shown in the Fig. 2. Calibration of the temperature was checked by determining the transition temperature of pure completely hydrated DPPC in water at pH 6 (41°C). Spectra were recorded each degree in the transition region and each two or five degrees outside the transition region. The scattered light, detected at right angle from the incident light, was collected on the photocathode of a cooled photomultiplier and amplified by a dc operational amplifier.

The temperature curves were determined from low to high temperatures. The estimated error in the calculation of the peak height intensities ratios made by amplitude measurements is ± 0.03 for the I<sub>2880</sub>/I<sub>2850</sub> peak intensities ratio and ± 0.08 for the I<sub>1068</sub>/I<sub>1098</sub> and I<sub>1128</sub>/I<sub>1098</sub> peak intensity ratios. The baseline was taken by drawing a straight line between 2800 and 3000 cm<sup>-1</sup> and between 1000 and 1200 cm<sup>-1</sup> as illustrated in Figs. 2a and 2b, respectively. A

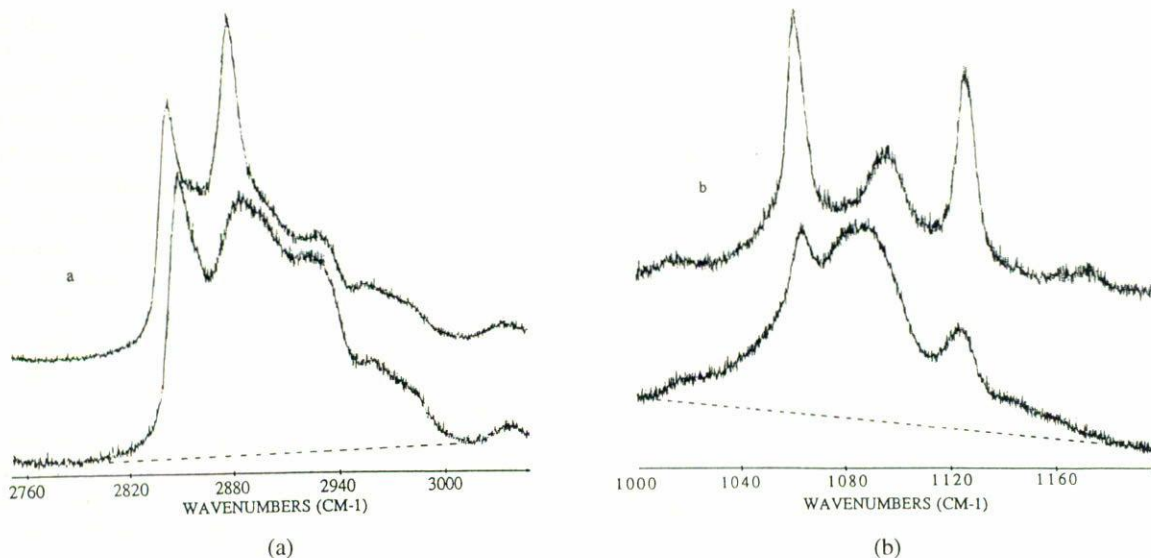


FIGURE 2. Raman spectra of the CH stretching modes, a) and C–C skeletal modes, b) at 10°C (lower) and 45°C (upper) of a DPPC aqueous solutions at pH 6.

systematic error could be made in the ratio calculation due to the presence of antibiotic specially for the more concentrated samples. As these antibiotics are not soluble in water, it is then impossible to subtract the antibiotic spectrum in solution and this correction has not been done. The Raman spectrum of both antibiotics powder does not have CH<sub>2</sub> stretching band at 2850 cm<sup>-1</sup> (spectrum not shown), the main bands in the  $\nu_{\text{CH}}$  region are at 2880 and 2935 cm<sup>-1</sup> and are mainly due to methyl CH<sub>3</sub> stretching modes. As the band at 2850 cm<sup>-1</sup> is only due to CH<sub>2</sub> stretching (and Fermi resonance) of the DPPC chains, the  $I_{2880}/I_{2850}$  ratio we measured may probably be over-estimated for the mixtures.

### 3. Results

It is well known that phospholipids and surfactants can exist in two states. In the solid ordered state at lower temperature, the hydrocarbon chains of the molecules rotate about their axes but are rigidly aligned. At higher temperature, a liquid-crystalline or disordered state is formed in which the chains have a liquid-like flexibility. Raman scattering and FTIR are powerful and non-invasive techniques to explore the organization of biological molecules. They provide informations about the thermotropic state transition occurring in surfactants, in lipids or in model membranes.

Raman spectra were studied in the 2750–3050 cm<sup>-1</sup> and 1000–1200 cm<sup>-1</sup> ranges. Analysis of the 2750–3050 cm<sup>-1</sup> region, which includes the contribution of the methyl and methylene CH stretching modes and Fermi resonances arising from interactions of the CH<sub>2</sub> stretching modes with the overtones of the CH<sub>2</sub> bending modes (1430–1460 cm<sup>-1</sup>), provides information on the perturbations arising in the hydrophobic core of the membrane and on the chain packing. In this region we observe two main bands at 2850 and

2880 cm<sup>-1</sup> which are the symmetrical and antisymmetrical CH<sub>2</sub> stretching modes respectively. The 1000–1200 cm<sup>-1</sup> region includes the antisymmetrical (1060 cm<sup>-1</sup>) and symmetrical (1130 cm<sup>-1</sup>) C–C stretching modes (skeletal modes) and provides information on the intrachain disorder with the band at 1098 cm<sup>-1</sup> representative of gauche bonds.

The use of FTIR spectroscopy, and the analysis of the stretching modes of carboxyl groups (1650–1800 cm<sup>-1</sup>) and phosphate and N<sup>+</sup>(CH<sub>3</sub>)<sub>3</sub> groups (900–1300 cm<sup>-1</sup>) of DPPC multilayers has allowed us to characterize the perturbations induced by Las-Na in the polar and interfacial regions of the membrane. Bands arising from the interfacial and polar region provide important information concerning bilayer hydration. In this analysis, the ester C=O band of DPPC is particularly useful because it is composed of two overlapping bands near 1740 and 1727 cm<sup>-1</sup>. It was originally suggested that they result from the sn-1 and sn-2 non-equivalent C=O groups [21]. New experiments have shown the high frequency band may represent “free” C=O groups, while the lower frequency band arises from hydrogen bonded C=O groups [22]. The DPPC absorption spectrum exhibits also two main features with maxima at 1242 and 1091 cm<sup>-1</sup>. These bands are attributed respectively to the antisymmetrical and symmetrical stretching modes of phosphate groups. Another signal appears as a shoulder at 1065 cm<sup>-1</sup> and is probably due to the R–O–P–R’ vibration [23]. The band at 1168 cm<sup>-1</sup> and the shoulder at 1180 cm<sup>-1</sup> are due to the C–O single bond stretching modes in the non-planar conformation of the C–C(=O)–O–C group respectively [24]. A band near 970 cm<sup>-1</sup> is due to the choline vibration  $\nu[\text{N}^+(\text{CH}_3)_3]$ .

It is known that hydration of DPPC [26–29] with mechanical agitation in excess water produces a suspension of “onion-like” multilamellar vesicles that undergo a sharp order-disorder transition at 41°C. When melting occurs, the

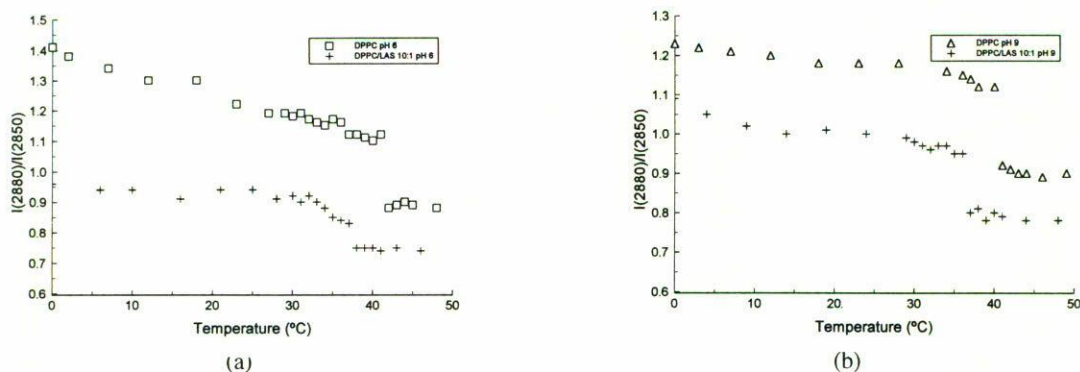


FIGURE 3. a) Temperature profile of DPPC and DPPC/Las-Na 10:1 molar ratio in water at pH 6, constructed from the  $I_{2880}/I_{2850}$  ratio. b) Temperature profile of DPPC and DPPC/Las-Na 10:1 molar ratio in water at pH 9, constructed from the  $I_{2880}/I_{2850}$  ratio.

antisymmetrical methylene CH stretching mode intensity decreases in relation to the symmetrical one. The peak height-intensity ratio  $I_{2880}/I_{2850}$  measures lateral interactions of adjacent chains and permits to characterize the chain packing and perturbations induced in the lipid chain organization. At the same time, changes occur in the C–C stretching modes region. At temperatures above  $T_m$ , the symmetrical and antisymmetrical C–C stretching modes become smaller than the band due to gauche conformations [28]. The peak height ratios  $I_{1069}/I_{1098}$  or  $I_{1128}/I_{1098}$  therefore reflect the trans/gauche isomerisation along the lipid chain.

For all the mixtures studied, in order to have quite clear figures, we do not present the results at different concentrations. Only the temperature profiles of DPPC and DPPC/antibiotic at 10:1 molar ratio constructed with  $I_{2880}/I_{2850}$  peak intensity ratio are presented. The results concerning the C–C stretching modes are summarized in the Tables I and II.

We first present and discuss our experimental results about DPPC model membranes in different water solutions containing DPPC/antibiotic mixtures, then results about CTAB/antibiotic solutions.

### 3.1. Raman spectrum of DPPC/Las-Na model membranes

#### 3.1.1. Solutions in water at pH 6

Figure 3a represents the temperature profiles formed from the  $I_{2880}/I_{2850}$  ratio, for DPPC and DPPC/Las 10:1 molar ratio in water at pH 6. As shown on this figure and in accordance with previous results [28, 29], the pure DPPC in water at pH 6 undergoes two transitions, the first one at 35°C (the so-called pretransition) and a cooperative transition found at 41°C (the main transition). Although the Raman intensity parameter is not very precise, a small discontinuity is always observed near 35°C. This transition involves a change from the lamellar gel ( $L_{\beta'}$ ) to the so-called rippled ( $P_{\beta'}$ ) phase. The second one is from the ripple to the fluid liquid crystalline ( $L_{\alpha}$ ) phase. At 10°C the  $I_{2880}/I_{2850}$  ratio equals 1.35 and then de-

TABLE I. Peak height intensity ratio of the skeletal vibration modes in Raman scattering below and above the main transition for the different DPPC/Las-Na samples and main transition temperatures.

Samples	$I_{1068}/I_{1098}$		$I_{1128}/I_{1098}$		$T_m$ (°C)
	35°C	44°C	35°C	44°C	
DPPC/water pH 6	1.25	0.86	1.02	0.53	41
DPPC/water pH 9	1.25	0.79	1.00	0.48	41
DPPC/Las 50:1 water pH 6	1.21	0.81	1.00	0.64	41
DPPC/Las 50:1 water pH 9	1.15	0.85	1.05	0.51	39
DPPC/Las 28:1 water pH 6	1.12	0.81	0.86	0.63	38
DPPC/Las 28:1 water pH 9	1.03	0.84	0.72	0.60	38
DPPC/Las 10:1 water pH 6	1.03	0.94	0.67	0.66	37
DPPC/Las 10:1 water pH 9	1.02	0.82	0.60	0.50	38

creases to nearly 1.1 at the pretransition, and remains constant till the main transition. The ratio remains constant at 0.90 above the main transition.

With the addition of the antibiotic, at pH 6, the pretransition of the DPPC multilayers is not observed for any of the molar ratios. The main transition temperature  $T_m$  practically the same as DPPC in water at pH 6 for the 100:1 and 50:1 lipid/Las-Na molar ratios but is reduced by  $\sim 3^\circ\text{C}$  for the 28:1 lipid/Las-Na molar ratio and reduced by  $4^\circ\text{C}$  for the 10:1 molar ratio as we can see in Table I. This effect has already been shown by DSC [19]. In the temperature range below the main transition (10°C–40°C), the addition of the antibiotic causes a significant decrease in the intensity ratio the  $I_{2880}/I_{2850}$  which drops, at 10°C from 1.3 in DPPC to 1.0 in the mixtures and at 35°C from 1.1 to 0.9 for all concentrations. At temperatures above the main transition, this ratio is nearly 0.75 for all DPPC/Las-Na mixtures, significantly smaller than the ratio obtained with DPPC in water (0.90). Addition of Las-Na in the DPPC multilayers increases slightly the proportion of gauche bonds for temperatures below the order-disorder transition temperature as it can be seen with the intensity ratios given in Table I. Above the main tran-

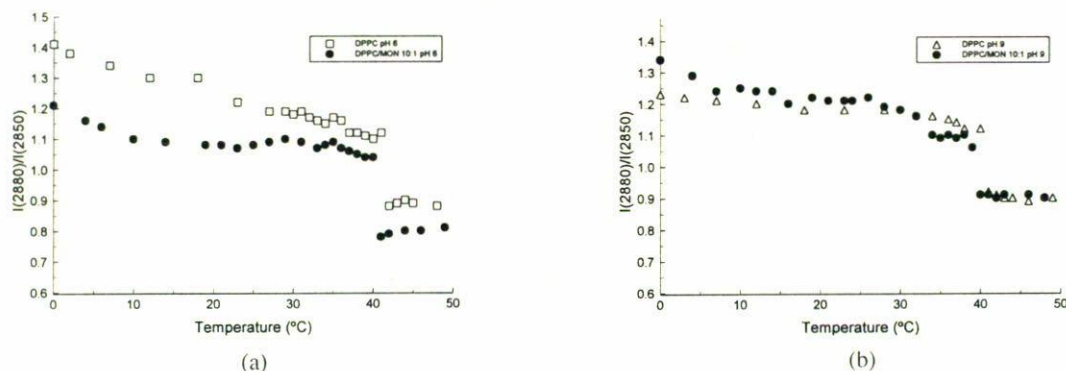


FIGURE 4. a) Temperature profile of DPPC and DPPC/Mon-Na 10:1 molar ratio in water at pH 6, constructed from the  $I_{2880}/I_{2850}$  ratio. b) Temperature profile of DPPC and DPPC/Mon-Na 10:1 molar ratio in water at pH 9, constructed from the  $I_{2880}/I_{2850}$  ratio.

sition, the intensity ratios are not very different from those of pure DPPC. The antibiotic strongly perturbs the DPPC bilayer with an increase of the fluidity above and below the main transition.

### 3.1.2. Solution in water at pH 9

Figure 3b represents the temperature profiles formed from the  $I_{2880}/I_{2850}$  ratio for DPPC and DPPC/Las-Na 10:1 molar ratio in water at pH 9. We can observe that no strong change appears on the pure DPPC profile except that the pretransition is not observed. The transition temperature is the same as in water at pH 6 as observed by previous results [22, 30]. The chain packing above the main transition as observed on the temperature profiles is not strongly modified by the pH change. The trans-gauche isomerisation as reflected by the  $I_{1068}/I_{1098}$  ratio is not really modified (Table I). As observed by Bartucci *et al.* [31], a small lateral expansion of the lipids can occur due to a screening effect. This expansion induces the hydrocarbon chains to tilt already in the gel state, and this could be the reason for the absence of the pretransition.

As we can see on Fig. 3b and in Table I, perturbations of DPPC bilayer also exist at pH 9. The main transition temperature is reduced by 2°C for the 100:1 and 50:1 lipid/Las-Na molar ratios. In all cases no pretransition is observed. For both 28:1 and 10:1 molar ratios the main transition temperature is reduced by 3°C and strong perturbations appear in the chain packing of the lipid-antibiotic mixtures. Below the main transition, at 35°C, the  $I_{2880}/I_{2850}$  intensity ratio is near 1 and drops to near 0.9 above the main transition temperature for the two lowest concentrations and to 0.8 for the highest concentration. Below the main transition the proportion of gauche conformers remains higher for the samples containing Las-Na than for pure DPPC solution.

It must be noticed that above the main transition the  $I_{2880}/I_{2850}$  ratio is the same for pure DPPC and the 50:1 and 28:1 molar ratios. The strong perturbation still exists in the gel phase but not exist in the liquid crystalline phase except for the highest Las-Na concentration (10:1 molar ratio).

## 3.2. Raman spectrum of DPPC/Mon-Na model membranes

### 3.2.1. Solutions in water at pH 6

A quite different behavior is found with DPPC/Mon-Na mixtures. As we can see on Fig. 4a, the main transition temperature is the same as DPPC for all concentrations.

The  $I_{2880}/I_{2850}$  ratio for the samples 50:1 and 28:1 is near 1.2 at 10°C, and goes to 0.9 at 35°C and 0.8 at 45°C while for the 10:1 sample it is 1.1 at 10°C, goes to 1.0 at 35°C and to 0.8 at 45°C. In the low temperature phase it seems that the higher concentrated sample induced a stronger perturbation than the other samples. In the high temperature phase (liquid crystalline phase), the chain packing seems decrease slightly for all samples with respect to DPPC. No difference in the trans/gauche isomerisation is observed between the different samples (Table II).

### 3.2.2. Solutions in water at pH 9

At pH 9 (Fig 4b), the main transition is still the same as pure DPPC at pH 9 and the pretransition is not observed. The  $I_{2880}/I_{2850}$  ratio is 1.2 at 10°C, nearly 1.1 at 35°C and 0.9 at 45°C for all concentrations. In the high temperature phase the chain packing is quite higher than in water at pH 6 and identical to the pure DPPC one. As mentioned above at pH 6, no difference is seen in the trans/gauche isomerisation at pH 9 (Table II).

## 3.3. Infrared absorption spectrum of DPPC/antibiotics mixtures

The infrared absorption spectrum in the 1300–900  $\text{cm}^{-1}$  spectral range is used to monitor the vibrations associated with the phosphate and choline groups in the polar part of the membrane. Modification of the pH of the water solution does not significantly change the infrared absorption spectrum of DPPC neither in this region nor in the polar part (1800–1650  $\text{cm}^{-1}$ ) (spectrum not shown).

TABLE II. Peak height intensity ratio of the skeletal vibration modes in Raman scattering below and above the main transition for the different DPPC/Mon-Na samples and main transition temperatures.

Samples	$I_{1068}/I_{1098}$		$I_{1128}/I_{1098}$		$T_m$ (°C)
	35°C	44°C	35°C	44°C	
DPPC/water pH 6	1.25	0.86	1.02	0.53	41
DPPC/water pH 9	1.25	0.79	1.00	0.48	41
DPPC/Las 50:1 water pH 6	1.15	0.78	0.99	0.52	41
DPPC/Las 50:1 water pH 9	1.21	0.80	1.01	0.51	41
DPPC/Las 28:1 water pH 6	1.15	0.82	1.00	0.55	41
DPPC/Las 28:1 water pH 9	1.20	0.91	1.16	0.55	41
DPPC/Las 10:1 water pH 6	1.12	0.77	0.99	0.60	41
DPPC/Las 10:1 water pH 9	1.19	0.80	1.01	0.56	40

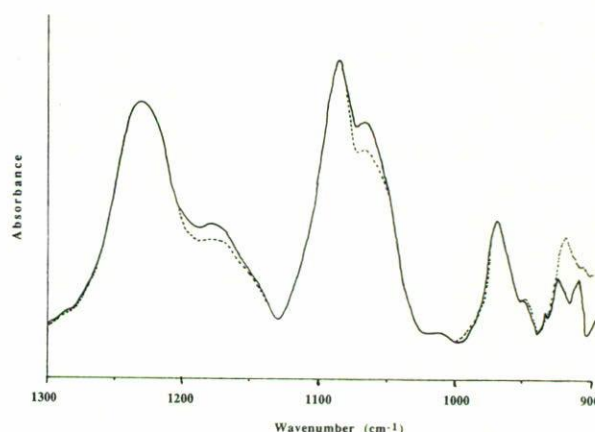


FIGURE 5. Infrared absorption spectrum in the 1300-900  $\text{cm}^{-1}$  region of DPPC (full line), DPPC/Las-Na 10:1 (dotted line) in pH 6 water solution in the high temperature phase (47°C).

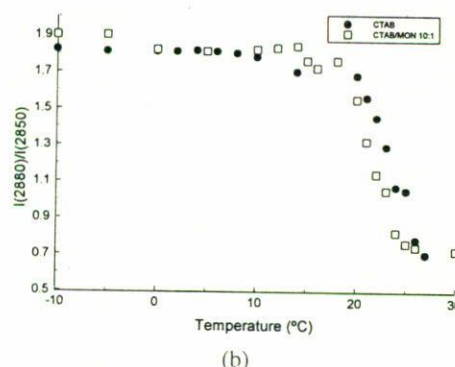
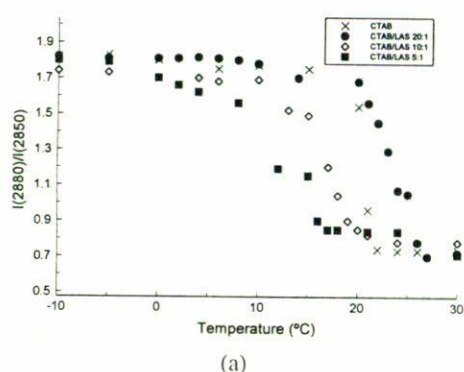


FIGURE 6. a) Temperature profile of CTAB and CTAB/Lasalocid in water at pH 6, for CTAB/Lasalocid 50:1, 20:1, 10:1 and 5:1 molar ratios, constructed from the  $I_{2880}/I_{2850}$  ratio. b) Temperature profile of CTAB and CTAB/Monensin for CTAB/Monensin 10:1 molar ratio in water at pH 6, constructed from the  $I_{2880}/I_{2850}$  ratio.

With addition of antibiotics, at pH 6 and at pH 9 for all molar ratios, no change is observed compared to DPPC water solution in the interfacial region of the phospholipid membrane with both antibiotics. But, very small changes are observed in the polar region (Fig. 5). These changes concern the shoulders near  $1069 \text{ cm}^{-1}$  (R-O-P-R' group) and near  $1180 \text{ cm}^{-1}$  (C-C(=O)-O-C group) only for DPPC/Las-Na mixtures. Intensity of both vibrations is concentration dependent. The intensity decreases as the concentration of antibiotic increases (spectrum not shown).

### 3.4. Raman spectrum of CTAB/antibiotics solutions

On Fig. 6a, we can see the results obtained with CTAB/Las-Na solutions at pH6. At 50:1 molar ratio we do not observe any change compared with the profile of a pure solution of CTAB, the transition temperature is near  $23^\circ\text{C}$ . When the concentration of antibiotic increases, the transition temperature is shifted to low temperatures. At higher concentration

we have found the transition at  $18^\circ\text{C}$  for the 10:1 molar ratio and at  $14^\circ\text{C}$  for the 5:1 molar ratio. We do not observe important changes of the intensity ratio in the low and high temperature phases compared to pure CTAB solution.

With Mon-Na, at pH 6, we do not observe any change in the transition temperature for the two highest molar ratios, but with 10:1 and 5:1 molar ratios the transition temperature is shifted to  $21^\circ\text{C}$  (Fig. 6b). Chain order is the same as in CTAB solution at low and high temperatures.

At pH 9, we do not observe any significant change with the results obtained at pH 6.

## 4. Discussion

The main result of this work is that these two molecules belonging to the same group of antibiotic ionophores have not the same effect on in vitro biological membranes. A careful observation of the experimental results and the structure of both molecules may provide a clue to this behavior.

In DPPC, the large molecular area of phosphorylcholine allows an expansion of the hydrocarbon chain matrix in the liquid crystalline state without disruption of the head-group lattice. In presence of excess water, the two-dimensional head-group contact no longer exists because water molecules can act as spacers molecules forming lateral bridges between the head-groups [32]. It means that in the liquid crystalline phase of DPPC, the value of 0.90 for the  $I_{2880}/I_{2850}$  ratio characterizes this two-dimensional arrangement. The fact that we found a lower value (0.75) for DPPC/Las-Na samples at pH 6 and 9, value very near of that obtained with liquid alkanes or surfactant micellar solutions, seems to indicate that hydrocarbon chains have more space than in pure DPPC solution and that lateral interchain interactions decrease. Below the order-disorder transition, a strong perturbation of the chain packing is also observed, without modification of the infrared absorption spectrum excepted on the vibrational bands due to the R-O-P-R' and C(=O)-O-C groups. With Lasalocid, the shift of the main transition temperature is concentration dependent. All these results suggest that Lasalocid molecules are inside the hydrophobic core of the DPPC membrane and interact with DPPC molecules. This interaction may occur between the lateral hydrophobic chain of Lasalocid and the DPPC chains. This interaction modifies the head-group lattice and causes an expansion of the hydrocarbon chain matrix which shifts the main transition to lower temperatures.

As we have seen, the fluidity of the gel phase is greater at pH 6 than at pH 9. At the same time, the number of gauche conformers is smaller at pH 9 than at pH 6. These results suggest a possible change in the conformation of Lasalocid. This could be possible by the liberation of the cation and the elongation of the Lasalocid molecules. In this case, the Las molecules stay in the hydrophobic core of the membrane with the COO- group near the interfacial region and produce a conformational change of the DPPC backbone which is observed by Infrared absorption. This is in agreement with the results of Hasmonay *et al.* [17] which have shown, using surface pressure techniques, that Las-Na molecules have an effect on Langmuir films of DPPC.

The same situation would occur with CTAB micelles where the transition temperature is lowered when the con-

centration of Lasalocid is increased. The local changes in the surface charge of the micelles could be the cause of the aggregation process above mentioned.

Since the results are very different, we must suppose that Monensin has not the same location as Lasalocid. Following Jain and Wu [33], since the methyl end region of the lipid bilayer is in relative state of disorder, a molecule localized in this region would have little or no effect on the transition profile. Thus, Monensin molecules would be very deeply buried in the hydrophobic core of the membrane probably between the terminal methyl groups of each monolayer. It would be the same with CTAB micelles. However this location of Monensin molecules does not explain why these molecules are not soluble in anionic surfactants and how the aggregation process we observed in CTAB solutions occurs. If Monensin molecules penetrate deeply in the hydrophobic core these effects would not exist, on the contrary, these effects would be in agreement with a molecule near the polar or the interfacial regions of the lipid.

It is known that stability constants of Monensin complexes are relatively much higher than those of Lasalocid in the same solvents. The smaller Lasalocid molecule is less stable than Monensin molecule [34]. The Monensin molecules would be near the interfacial region of the membrane probably in a neutral form to prevent any bonding with the polar head of the lipids. The interaction would be electrostatic explaining the absence of modification of the thermotropic properties of the DPPC membranes and CTAB micelles with Monensin.

In any case, as the changes observed are very small at relatively high concentrations, at physiological levels, none of the antibiotics produce sensitive modification of the thermotropic properties of biological membranes.

## Acknowledgments

Thanks are due to Dr. C. Betrencourt and Prof. M. Gardès from the Université René Descartes and Prof. E. Haro-Poniatowski from the Universidad Autónoma Metropolitana (UAM) for helpful and stimulating discussions.

- 
- \* On leave from: Groupe de Recherche en Physique et Biophysique (GRPB), Université René Descartes, UFR Biomédicale, 45 rue des Saints-Pères, 75270 Paris Cedex 06, France.
1. S.M. Johnson, J. Herrin, S.J. Liu, and I.C. Paul, *J. Am. Chem. Soc.* **92** (1970) 4428.
  2. P.G. Schmidt, A.H.J. Wang, and I.C. Paul, *J. Am. Chem. Soc.* **96** (1974) 6189.
  3. I. Suh, K. Aoki, and H. Yamazaki, *Inorg. Chem.* **28** (1989) 358.
  4. I. Suh, K. Aoki, and H. Yamazaki, *Acta Cryst.* **C45** (1989) 415.

5. K. Aoki *et al.*, *J. Am. Chem. Soc.* **114** (1992) 5722.
6. G.R. Painter, R. Pollack, and B.C. Pressman, *Biochemistry* **21** (1982) 5613.
7. A. Chattopadhyay, S.S. Komath, and B. Raman, *Biochim. Biophys. Acta* **1104** (1992) 147.
8. P. Malfreyt, Y. Pascal, and J. Juillard, *J. Chem. Soc. Perkin Trans.* **2** (1994) 2031.
9. J. Bolte *et al.*, *Can. J. Chem.* **60** (1982) 981.
10. E. Fernández, J. Grandjean, and P. Laszlo, *Eur. J. Biochem.* **167** (1987) 353.

11. Y.N. Antonenko and L.S. Yaguzhinsky, *Biochim. Biophys. Acta* **938** (1988) 125.
12. J. Juillard, C. Tissier, and G. Jeminet, *J. Chem. Soc. Faraday Trans. 1* **84** (1988) 951.
13. Y. Pointud and J. Juillard, *J. Chem. Soc. Faraday Trans. 1* **84** (1988) 959.
14. P. Laubry, C. Tissier, G. Mousset, and J. Juillard, *J. Chem. Soc. Faraday Trans. 1* **84** (1988) 969.
15. G. Painter and B.C. Pressman, *Biochem. Biophys. Res. Commun.* **97** (1980) 1268.
16. F.J. Aranda and J.C. Gómez-Fernández, *Biochim. Biophys. Acta* **860** (1986) 125.
17. H. Hasmonay *et al.*, *Biochim. Biophys. Acta* **1193** (1994) 287.
18. A. Hochapfel, H. Hasmonay, and P. Peretti, *Mol. Cryst. Liq. Cryst.* **270** (1995) 23.
19. C. Betrencourt *et al.*, *Mol. Cryst. Liq. Cryst.* **262** (1995) 179.
20. J.A. Tarbin and G. Shearer, *J. Chromatography* **579** (1992) 177.
21. E. Mushayakarara and I.W. Levin, *J. Phys. Chem.* **86** (1982) 2324.
22. A. Blume, W. Hübner, and G. Messner, *Biochemistry* **27** (1988) 8239.
23. J.R.L. Arrondo, F.M. Goñi, and J.M. Macarulla, *Biochim. Biophys. Acta* **794** (1984) 165.
24. U.P. Fringeli and H.H. Günthard, *Membrane Spectroscopy, Molecular Biology, Biochemistry and Biophysics*, Vol. 31 (Springer-Verlag, Berlin, 1981) p. 270.
25. A. Hochapfel, H. Hasmonay, M. Jaffrain, and P. Peretti, *Mol. Cryst. Liq. Cryst.* **215** (1992) 221.
26. J.L. Lippert and W.L. Petitcolas, *Proc. Natl. Acad. Sci. USA* **68** (1971) 1572.
27. L.J. Lis, J.W. Kauffman, and D.F. Shriver, *Biochim. Biophys. Acta* **406** (1975) 453.
28. N. Yellin and I.W. Levin, *Biochim. Biophys. Acta* **489** (1977) 177.
29. D.F.H. Wallach, S.P. Verma, and J. Fookson, *Biochim. Biophys. Acta* **559** (1979) 153.
30. M.S. Fernández, M.T. González-Martínez, and E. Calderón, *Biochim. Biophys. Acta* **863** (1986) 156.
31. R. Bartucci, N. Gulfo, and L. Sportelli, *Nuovo Cimento* **12** (1990) 1585.
32. H. Hauser, I. Pascher, R.H. Pearson, and S. Sundell, *Biochim. Biophys. Acta* **650** (1981) 21.
33. M.K. Jain and N.M. Wu, *J. Membrane Biol.* **34** (1977) 157.
34. B.G. Cox, N. Van Truong, J. Rzeszotarska, and H. Schneider, *J. Chem. Soc., Faraday Trans. 1* **80** (1984) 3275.